Surface structure determination of Pd ultrathin films on Ru(0001): Possible magnetic behavior

A. de Siervo,[1,*] E. De Biasi,[1] F. Garcia,[1] R. Landers,[1,2] M. D. Martins,[3] and W. A. A. Macedo[3]
[1]*Laboratório Nacional de Luz Síncrotron, 13084-971 Campinas, Brazil*
[2]*Instituto de Física Gleb Wataghin, Universidade Estadual de Campinas, 13083-970 Campinas, Brazil*
[3]*Laboratório de Física Aplicada, Centro de Desenvolvimento da Tecnologia Nuclear, 31270-901 Belo Horizonte, Brazil*
(Received 4 January 2007; revised manuscript received 13 May 2007; published 30 August 2007)

Nowadays, ultrathin films play a fundamental role in modern materials science and technology. Recently, several theoretical works indicate that the magnetic properties of Pd ultrathin films could be controlled by structural parameters of the film, and much work has been done to study induced magnetic properties of ultrathin Pd films grown on different substrates. For the epitaxy of Pd monolayers on Ru(0001), it was not clear if Pd grows in an hcp or fcc structure and a detailed surface structure determination was not available for this system. In this study, Pd films with thicknesses ranging from submonolayer up to approximately 15 ML were grown on a Ru(0001) single crystal substrate under UHV conditions, and the electronic structure, surface crystallography, and magnetism were investigated by multiple (experimental and theoretical) techniques: x-ray photoelectron spectroscopy and diffraction using conventional Mg $K\alpha$ and synchrotron radiation sources, low- and high-energy electron diffraction, magneto-optical Kerr effect measurements, and density-functional theory calculations. The electronic structure, surface crystallography, and magnetism of the Pd films are discussed in detail.

DOI: 10.1103/PhysRevB.76.075432 PACS number(s): 75.70.Rf, 79.60.Bm, 61.14.Qp, 71.15.Mb

I. INTRODUCTION

The study of thin metal films on oriented metal surfaces has been a very important research topic in surface science during the past decades. Some special systems involving transition metals and noble metals on selected surfaces have been exhaustively explored by both experimentalists and theoreticians, with the aim of developing new materials and to tailor selected physical and chemical properties. Specifically for the transitions metals from platinum group (Ni, Pd, and Pt) and noble metals (Cu, Ag, and Au), the major motivation for studying their surface alloys phases has come from the interest in creating, artificially, surfaces with enhanced chemical reactivity and selectivity for catalysts when compared to surfaces of homogeneous solids.[1] However, very little attention has been paid to the magnetic properties of these materials, especially ultrathin films of transition metals that are nonmagnetic in the bulk phase but can become magnetic as nanoparticles or films.

In almost all the cases, the physical and chemical properties of the films are strongly dependent on the electronic and atomic structures (i.e., positions of the atoms) in the film, which could be influenced by the substrate characteristics. Particularly, in magnetism, it is already well known that ultrathin films of nonmagnetic materials can show interesting magnetic properties when they are grown on some particular surfaces of magnetic materials or when they present distortion in its electronic or geometric structure.[2] Ultrathin fcc-like Fe films grown epitaxially on Cu(100) or Cu-based (100) alloy surfaces[3,4] are a model system where the structure and magnetism depend strongly on the growth conditions. Depending on the preparation mode, thickness, and/or growth temperature, it is possible to obtain ferromagnetic, antiferromagnetic, and/or nonmagnetic Fe films.[2–4] It is possible, for example, to induce ferromagnetism in nonferromagnetic materials such as Ag, Ru, Mo, and Pt, when they are ultrathin films sandwiched between Fe films.[5] It is also known that the film thickness and interface effects, such as alloy formation and charge transfer, are important in determining the final magnetic properties of the material which are undoubtedly correlated to its electronic structure. Notwithstanding, for many low-dimensional epitaxial systems with transition metal already explored in the literature, not all physical mechanisms were unambiguously determined.

Moreover, few experimental studies have explored the possibility of inducing intrinsic ferromagnetism in nonferromagnetic materials due to changes in the electronic and atomic structures produced in ultrathin films and in nanoparticles.[6–14] More recently, some theoretical predictions have vindicated the unusual possibility of inducing ferromagnetism in nonferromagnetic materials such as Rh, Pd, Ag, and Au by artificially changing their electronic structure or atomic arrangement[6,8,12] in such a way that the Stoner criterion for the ferromagnetism is satisfied.[15]

In fact, it is quite complicated to produce magnetic ordering and have at the same time noble metal characteristics because these are competing properties of the materials. The main characteristic of a noble metal and some transition metals is that the *d valence band* is filled or almost filled and situated well bellow the Fermi level. This is the main reason that noble metals have surfaces with low chemical activity. On the other hand, ferromagnetic order needs holes in the *d* valence band close to the Fermi edge to allow preferential spin alignment. In other words, a large density of states (DOS) near the Fermi level with different populations of the spin-up and spin-down states are needed.

From the basic fundaments, ferromagnetism is a consequence of the exchange interaction potential in a many-electron system. It does not depend on the electronic configuration of the atom itself, but on the density of electronic states at the Fermi energy, which is a collective effect determined by the electronic interactions between one particular atom and its neighbors in the crystalline structure. A simple

model for the description of transition metal ferromagnetism at limit of $T=0$ is the Stoner model,[15(a),15(b)] which treats the electron-electron interaction within the mean field approximation. To fulfill the Stoner criterion for ferromagnetism, $U \times N(E) > 1$ must be satisfied, where U is the Stoner parameter or Stoner-Hubbard parameter and $N(E)$ is the density of states at the Fermi level of the paramagnetic state. Here, it is important to clarify that Stoner criterion is one approximation valid for $T=0$, which is used in this paper together with density-functional theory (DFT) calculations for tailoring some conclusions regarding conditions to have ferromagnetic behavior on Pd.

In short, in some nonferromagnetic systems where the bulk phases are close to fulfilling the Stoner criterion, for example, Pd $[U \times N(E) \approx 0.8]$, it is possible, at least in theory, to produce ferromagnetism by changing and/or controlling its atomic and electronic structure. Experimentally, such a possibility of modification can be done artificially by growing the metal as nanoparticles or as ultrathin films on selected matrices and/or surfaces.

Another possibility to induce ferromagnetism in such a type of nonferromagnetic material is by changing the electronic structure of the atoms by the charge transfer effect, by deposition on adequate surfaces or interfaces. The effect was predicted by electronic structure calculations and experimentally observed in some selected cases of Pd, Ag, and Au nanoparticles capped with organic molecules which produced the necessary charge transfer in the atoms at the surface to display a ferromagnetic character.[7,10,11] In these cases, the ferromagnetism observed is attributed only to the surface atoms that have their electronic structure changed. Since the Stoner parameter U is related to the exchange interaction, and thus very little influenced by crystal symmetries, the changes in the density of states at the Fermi energy play a decisive role in establishing ferromagnetic ordering.

Another possibility to modify the DOS and induce ferromagnetic order is by changing the atomic arrangement of nonmagnetic atoms. Recently, theoretical predictions based on electronic band structure calculation and also on results from indirect magnetic measurements[6,8,9,12] claim that it is possible to induce a long range ferromagnetic order in Pd by changing the atomic symmetry through strong lattice expansions and/or by reductions in its coordination number, specially in an hcp packing. Changes in symmetry, bond length, and angles from the usual Pd structure would lead to more states with antibonding character at the Fermi level, which could produce the necessary increase of the $N(E)$ to fulfill the Stoner criterion.

Bulk Pd is fcc and does not show a layer-by-layer homoepitaxial growth in the (111) direction.[16] However, it is expected that Pd(111) can grow homoepitaxialy with Sb as a surfactant agent[17] and on some selected substrates, such as Ru(0001), C(0001), W(100), or Nb(100).[12,18–20] hcp Ru(0001) has an in-plane lattice parameter very close to that one displayed by the Pd(111) surfaces, and it is expected that Pd can grow almost in a planar fashion on this surface.[18–20] Previous results for the epitaxy of Pd on Ru(0001) indicate fully the layer-by-layer growth or only the partial (first two layers) layer-by-layer growth mode.[21,22] Nevertheless, the structure of the Pd monolayers on Ru(0001) is still an open question. Campbell *et al.*[26] and more recently Hoster *et al.*[25] speculate that the films have fcc structure, but without any structural determination. None of the previous works indicates clearly what type of crystalline structure Pd films form when grown on top of Ru(0001). The most interesting aspect is that there are indications in the previous works for a strong electronic interaction of the Pd atoms with the Ru(0001) surface. From the point of view of the film growth, we are expecting that a strong electronic interaction would favored an hcp growth of Pd on Ru(0001) and consequently opening the possibility for a ferromagnetic behavior on this system. We investigate here the possibility of inducing ferromagnetism in Pd films purely by electronic and symmetry effects. In this work, we have performed a detailed electronic and atomic surface structure determination for Pd monolayers grown on Ru(0001). We have explored the thickness range from 0.5 up to 15 ML Pd, deposited on the Ru(0001) substrate at room temperature (RT) and at 160 K [low temperature (LT)]. To investigate the structural and electronic properties, we have applied x-ray and synchrotron radiation photoemission (XPS, PES) and photoelectron diffraction (XPD), reflection high-energy and low-energy-electron diffraction (RHEED and LEED). The magnetic character of these films was investigated using *in situ* magneto-optical Kerr effect (MOKE) measurements and the experimental results were compared with simulations obtained by DFT calculations. Hence, this multitechnique study can contribute to the understanding of some unclear issues on the Pd/Ru(0001) system. Section II of this paper describes the experimental setups. The XPS, LEED, and RHEED results are presented in Sec. III. We present a detailed surface structure determination in Sec. IV, magnetic measurements and DFT calculations in Sec. V, and finally, Sec. VI contains our concluding remarks.

II. EXPERIMENT

The experiments were carried out in two independent ultrahigh vacuum systems equipped with very similar setups for *in situ* surface science studies, thin film growth under molecular beam epitaxy conditions, and structural and magnetic characterization. Both chambers were equipped with LEED optics, XPS, argon sputter ion gun, manipulator with heating and LN2 cooling ($\sim$160 K), and electron beam evaporators and operate at a base pressure lower than 2×10^{-10} mbar during the measurements. The XPD and PES measurements were performed at the Brazilian Synchrotron Light Laboratory (LNLS) using a bending magnet beamline with a spherical grating monochromator (SGM) and also using a conventional Mg $K\alpha$ radiation source. The surface science workstation was equipped with an electron analyzer (Omicron HA125HR with multidetection) with high energy and angle resolution, mounted in the plane of the storage ring and a high precision two axis manipulator, allowing sample heating up to 1500 K by electron bombardment, and cooling to 160 K. In this setup, it was also possible to monitor the growth process by continually measuring the XPS signal. For the RHEED and MOKE measurements, we used a second experimental setup at the Laboratory of Applied Physics/

CDTN also equipped with a high resolution electron analyzer (CLAM2, VG) and a dual Al/Mg $K\alpha$ radiation source. In this case, the development of the surface structure during the Pd deposition was monitored in detail with RHEED measurements. For the RHEED experiments, we used a 15 keV electron beam impinging on the sample surface at grazing incidence and the reflected and diffracted beams were recorded from a phosphor screen with a charge-coupled device camera. By evaluating the RHEED diffraction patterns, it was possible to extract precise information about the evolution of the Pd in-plane lattice parameter during the growth as well as to infer the growth mode through a careful analysis of the spot intensities.

The substrate, a high purity Ru(0001) single crystal, was cleaned in UHV by several cycles of argon ion sputtering (1.0 μA mm^{-2} at 500 eV) followed of annealing to 1000 K for 5 min, using an electron beam (20 mA, 1.3 keV) impinging on the backside of the crystal. The Ru (0001) surface was considered clean when contaminants such as C, O, N, and S were not detected by XPS and the LEED pattern displayed very sharp (1×1) spots, indicating atomically flat terraces. High purity (99.99%) Pd were deposited on the Ru(0001) at RT and LT from electron beam evaporation sources which were exhaustively degassed previously the experiment. The pressure during the Pd growth was 4×10^{-10} mbar and the deposition rate was 0.42 Å/min, as determined by XPS.[22]

For each Pd film, we performed the angle-scanned XPD measurements by varying the azimuth angle, in steps of 3° over a range of 120°, and generated the complete 360° azimuth pattern by replicating the data with threefold symmetry. Since the Ru(0001) displays a sixfold symmetry and Pd(111) conventionally shows a threefold symmetry, it is possible to guarantee that all features in the azimuth curves have been measured in the interval of 120°. The polar angle, defined as the angle between the analyzer axis and the surface normal, was varied from 0° (normal emission) to 78° in steps of 3°. The photoelectrons in the XPD measurements were excited with conventional Mg $K\alpha$ and synchrotron radiation of 700 eV.

III. RESULTS

A. X-ray photoelectron spectroscopy analysis

Different studies which claim layer-by-layer growth for Pd monolayers on a Ru(0001) substrate have been conducted by XPS or Auger electron spectroscopy.[18,20,26] For the Pd/Ru system, the monitoring of the most intense Auger transition is difficult due to the coincidences of the Pd and the Ru peaks.[18] We have followed the evolution of the XPS intensities of the Ru 3d (280.2 eV) and Pd 3d (335.6 eV) peaks measured at normal emission angle. An example of the intensity curves is shown in the Fig. 1. In a layer-by-layer or Frank–van der Merwe (FV) growth mode, abrupt changes are expected in the slope of the XPS intensity curves as a function of the evaporation time, each time a monolayer is completed. These breaks are clearly seen for the first three or four deposited monolayers in systems that grow in the FV mode, for example, Cu on Pd(111).[21] We repeated the growth process several times, with different deposition rates, at RT and at LT. For all cases, it was not possible to distinguish clearly a segmented curve for the XPS intensities of Pd and Ru as a function of the Pd thickness, i.e., we did not observe any evidence of layer-by-layer growth for Pd on Ru(0001) at RT or at LT.

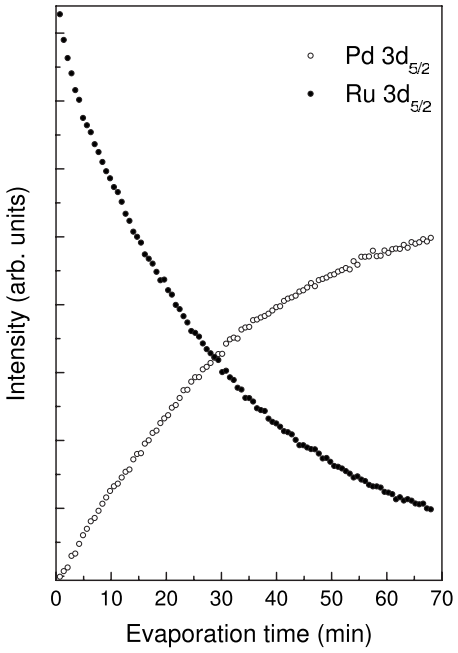

FIG. 1. Evolution of the XPS intensity for the Pd 3d (open circles) and Ru 3d (full circles) peaks as a function of the evaporation time for Pd grown on Ru(0001) at RT.

It is well known that contaminants can change the growth mode by acting either as nucleation centers that produce three dimensional islands or as surfactant that produces a FV growth mode. Despite the low pressures of $(3-4)\times10^{-10}$ mbar, always observed during the Pd evaporations, *a priori* it is not possible to rule out contamination as a possible explanation for the result obtained here when compared with previous investigations. We used the PES measurements with synchrotron light to check for contaminants in the films. Compared to the conventional x-ray sources, synchrotron light offers the advantage of a very small spot size and, obviously, tunable photon energy allowing the increase of the photoemission cross sections for the typical contaminants, and, therefore, increased sensitivity to very low concentration of contaminants. With exception of H, which cannot be measured directly by the XPS, the presence of any other contaminants in our Pd films was below the XPS detection limit, ruling out this possibility as a cause for the absence of layer-by-layer growth.

The evaporating flux was calibrated using the XPS attenuation of the Ru 3d intensity by applying an exponential model as described in Ref. 22. This result is in a very good agreement with the value obtained with angle-resolved x-ray photoelectron spectroscopy analysis.

Despite the fact that it was not possible to see a clear indication of a layer-by-layer growth, (1×1) LEED patterns with sharp spots were observed in all ranges of coverage (see Fig. 4). The combination of the XPS results and the LEED

observation strongly indicates that Pd shows a three-dimensional growth on Ru(0001).

In XPS, chemical shift can provide important indications of alloy formation, charge transferring, or changes in the electronic structure that could be correlated to initial- and/or final-state effects in the photoemission process. In Pd/Ru, the surface energies reported in the literature are 2.0 J m^{-2} for the Pd and 3.4 J m^{-2} for the Ru.[23] It is considered that Pd does not form an interfacial compound (surface alloy) when deposited on Ru(0001) surfaces. Diffusion or segregation processes are also not expected theoretically.[24] If alloy formation and diffusion and/or segregation processes occur changes in the relative intensities of the XPS peaks and in their binding energies (BEs) are expected to be observed upon annealing. No such experimental evidence was observed here or in previous results using XPS analysis.[26] Furthermore, atomic resolution scanning tunneling microscopy (STM) study of a submonolayer Pd film on Ru(0001) showed no indication at all of Ru-Pd exchange and its incorporation was also excluded in consequence of annealing studies.[25]

Thus, we can state that alloy formation and diffusion do not happen in Pd/Ru(0001) in the interval of LT up to at least 1000 K. If alloy formation is not present, we would expected no significant energy shifts in the XPS spectra, which is confirmed (constant BE) for the Ru photoelectron peaks [Figs. 2(b) and 2(d)]. However, we observe that the BEs of the Pd levels are strongly shifted to higher values, in agreement with previous results.[26] By fitting the spectra collected during the Pd growth [Fig. 2(a)], we can observe even for the very low coverage a shift in the Pd $3d_{5/2}$ peak of about 0.3 ± 0.1 eV when compared to the Pd bulk value of 335.1 eV, notwithstanding that our experimental resolution is not enough to clearly separate different spectral components. For the low coverage regime, more than one component is expected due to different adsorption sites, low coordination number, and different environments for the Pd atoms. First, in the very low coverage, Pd atoms interact directly with the Ru atoms at the surface and, in sequence, the Pd-Pd interaction is present. This shift progressively increases as a function of the film thickness to a maximum value of 0.6 ± 0.1 eV (around seven Pd monolayers), which is in very good agreement with previous results obtained with conventional Al $K\alpha$ x-ray source.[26] The presence of such a shift is not completely understood and could be correlated to different effects, including structural changes in the film, polarization, and hybridization of the d orbital in the valence band, and initial- and/or final-state effects during the photoemission process.[27] For high coverage, the Pd $3d$ BE tends to 335.3 ± 0.1 eV, a value close to the expected one for a clean Pd(111) surface (335.1 eV).

PES studies of Pd on Ru(0001) conducted by Andersen and co-workers[19,28,29] by using intermediate photon energy ($h\nu$=400 eV) indicate a binding energy of 335.08 eV for the Pd $3d_{5/2}$ at coverage around 4 ML. Although more than one spectral component is identified at low Pd coverage, the obtained binding energies are different from those presented here and in Ref. 26.

To clarify this discrepancy, synchrotron radiation ($h\nu$ =700 eV) and Mg $K\alpha$ XPS measurements have been done

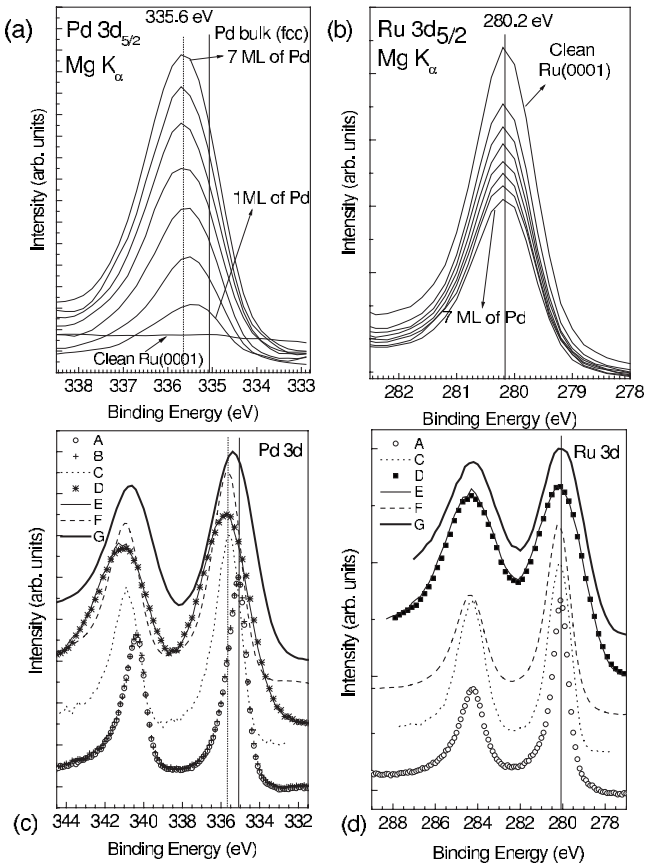

FIG. 2. XPS intensities for the Pd $3d$ (a) and Ru $3d$ (b) in normal emission simultaneously obtained during the growth. It is clearly noted the absence of shifts for the Ru $3d$ peaks and a progressive trend from 0.3 to 0.6 eV in the Pd $3d$ peaks as a function of the coverage. (c) and (d) show, respectively, Pd $3d$ and Ru $3d$ peaks for different cases of annealing, photon energy excitation, and substrate (details in the text).

for different Pd thicknesses deposited on Ru(0001) at RT and also after annealing at 1000 K. The PES and XPS results obtained after annealing helped us to discard the influence of surface contamination by residual gas and to rule out Pd-Ru alloy formation. Figure 2(c) compares several Pd $3d$ XPS spectra from Pd films on Ru(0001) and on Pd(111) as well as from the Pd(111) single crystal with different excitation energies and annealing [A, Pd(111) clean surface excited with Mg $K\alpha$; B, 7 ML of Pd on Pd(111)/Mg $K\alpha$; C, 4 ML of Pd on Ru(0001) after annealing at 1000 K (better resolution)/$h\nu$=700 eV; D, 4 ML of Pd on Ru(0001) as grown/$h\nu$ =700 eV; E, 4 ML of Pd on Ru(0001) after annealing at 1000 K/$h\nu$=700 eV; F, 7 ML of Pd on Ru(0001) as grown/Mg $K\alpha$, G, high coverage (~15 ML) as grown/$h\nu$=700 eV]. Independent of the excitation energy or annealing, the Pd films on Ru(0001) display a positive shift of about 0.5 eV in comparison with the Pd(111) which present a BE of 335.1 eV. In contrast, the binding energy of the Ru $3d$ is constant in 280.2 eV, as shown in Fig. 2(d) (it is shown the equivalent Ru $3d$ curves for the cases A, C, D, E, F, and G discussed above). Both synchrotron radiation and conventional x-ray sources determinations agree. BE determination

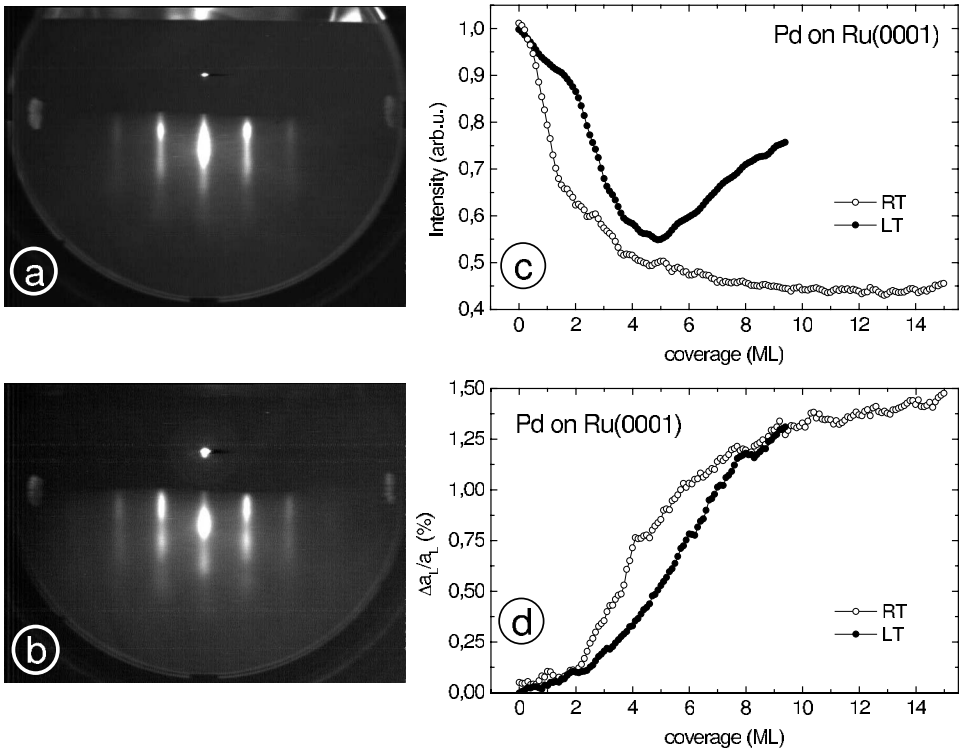

FIG. 3. RHEED measurements for Pd deposition on Ru(0001) at LT and RT. Typical RHEED patterns at 15 keV are shown for the clean Ru(0001) surface (a) and for approximately 15 ML of Pd (b). The RHEED intensity profile as a function of the Pd coverage (c) does not indicate FV growth even at RT. The evolution of the in-plane lattice parameter as a function of the Pd coverage is shown in (d) for RT and LT growths.

obtained in the second chamber (for RHEED experiments) agree also with the values obtained here. It might be that different methods of sample preparation or calibrations of the photon energies or electron analyzer led to the discrepancies in the values of the absolute Pd 3*d* BE in Pd/Ru presented in Refs. 19, 28, and 29.

B. Reflection high-energy electron deffraction analysis

The growth of Pd on Ru(0001) was also observed by RHEED in order to determine the growth mode and the evolution of the Pd in-plane lattice parameter as a function of the thicknesses of the Pd films, deposited at room temperature and also at 160 K. The procedure used in the RHEED analysis is described in the Ref. 21.

RHEED patterns for the clean Ru(0001) surface and for 15 ML Pd Ru(0001) at RT are shown in the Figs. 3(a) and 3(b), respectively. Despite the good quality of the LEED (see Fig. 4) and the RHEED patterns after Pd deposition, no RHEED oscillations were observed for both RT and LT growths. The RHEED intensity is shown as a function of the Pd coverage in Fig. 3(c) for RT deposition. For LT growth, LEED and RHEED results strongly suggest three-dimensional growth mode that could be related to a decrease in the atom mobility and/or due to an increase in the surface energy barrier.[16] For both growth conditions, our results extracted from XPS and RHEED analysis do not clearly indicate the layer-by-layer growth. It is one indication that the growth mode probably is not a true layer-by-layer growth. However, the absence of segments in the XPS curves or intensity oscillations in the RHEED curves does not allow excluding layer-by-layer growth. A step flow growth mode, for example, does not produce RHEED intensity oscillations or a segmented XPS curve. Further investigations including STM analysis are desirable for an unquestionable determination of the growth process in this system.

Figure 3(d) shows the relative change in the in-plane lattice parameter in Pd/Ru(0001), which increases from the value presented by the Ru single crystal to a value 1.2% larger at 8 ML, and then tends to a 1.5% expansion for a Pd coverage around 15 ML. This expansion is almost exactly the difference between the in-plane lattice parameter of pure Pd(111) and the Ru(0001). Independent of the growth temperature (RT or LT), for the first two Pd ML, the in-plane lattice parameter is almost identical to the Ru(0001) substrate. We conclude that Pd grows pseudomorphic with the substrate only for the first monolayer. This system presents large Pd three-dimensional structures but does not represent a genuine FV growth mode. The influence of contaminants in the growth mode was ruled out from a careful XPS analysis of the surfaces before and after Pd deposition.

IV. SURFACE STRUCTURE DETERMINATION

XPS indicates that Pd strongly interacts with the Ru(0001) surface, however, not producing an alloy. Such interaction could be correlated with the atomic structure of the film. RHEED indicates a Pd film with in-plane lattice parameter rapidly relaxed to the bulk value; also in Fig. 3(b), evidence for three dimensional growth can be seen. Figure 4 shows the LEED patterns for different Pd films grown on Ru(0001) and compares them to the LEED patterns of clean Ru(0001) and Pd(111) surfaces. The Pd films display very similar patterns to the one of the clean Ru(0001) with a possible sixfold symmetry in contrast with the clear threefold symmetry of the Pd(111).

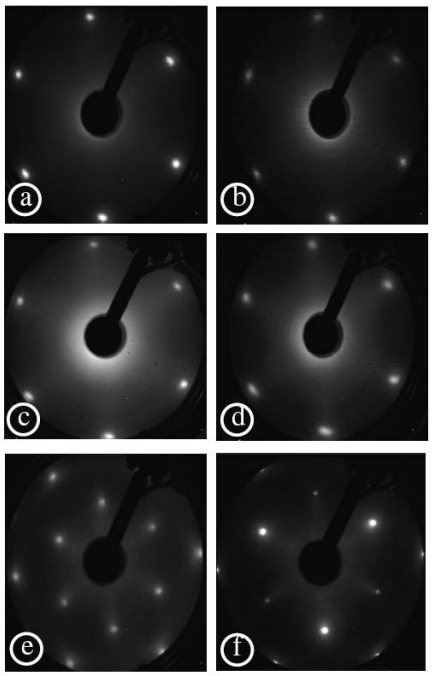

FIG. 4. LEED patterns collected at RT with primary electron energy of 59 eV [(a)–(d)] and 145 eV [(e) and (f)] . (a) Clean Ru(0001), (b) 5 ML of Pd on Ru(0001) as grown, (c) 5 ML of Pd on Ru(0001) annealed to 700 K, [(d) and (e)] 15 ML of Pd on Ru(0001) as grown, and (f) clean Pd(111) single crystal (details in the text).

To better understand the local atomic ordering of these films, systematic angle-scanned XPD experiments were carried out for the films with coverage ranging 0.5–15 ML. Figure 5 shows the experimental XPD patterns for the Pd and Ru emitters excited with Mg $K\alpha$ for different Pd film thickness as grown on Ru(0001) at RT. The left column presents Pd $3d_{5/2}$ patterns and the right column Ru $3d_{5/2}$ patterns for 0.5–1.0 ML [(a) and (b)], 5–6 ML [(c) and (d)], and 15 ML [(e) and (f)]. In the left corner of each pattern, the maximum anisotropy of the signal is shown, in percent, which indicates the maximum relative variation of the intensities in the diffraction pattern. The diffraction pattern of Fig. 5(a) exhibits bright spots almost only for polar angles higher than 60° and with sixfold symmetry. From this observation, we can directly learn that Pd is located only at the surface and has not diffused into the substrate, confirming the XPS results. For higher coverage of Pd, 5–6 ML [Fig. 5(b)] and 15 ML [Fig. 5(c)], the XPD patterns clearly exhibit sixfold symmetry. However, it is not possible to conclude directly from these patterns about the atomic arrangement of the atoms. Several possibilities can be suggested to explain such a pattern, for example, Pd packing in an hcp structure, or in a fcc structure with several stacking faults, or even as Pd islands in rotated domains.

To perform a careful atomic structure analysis, we have been used a theory-experiment comparison between the XPD experiments and simulations based on a comprehensive multiple scattering calculation photoelectron diffraction approach.

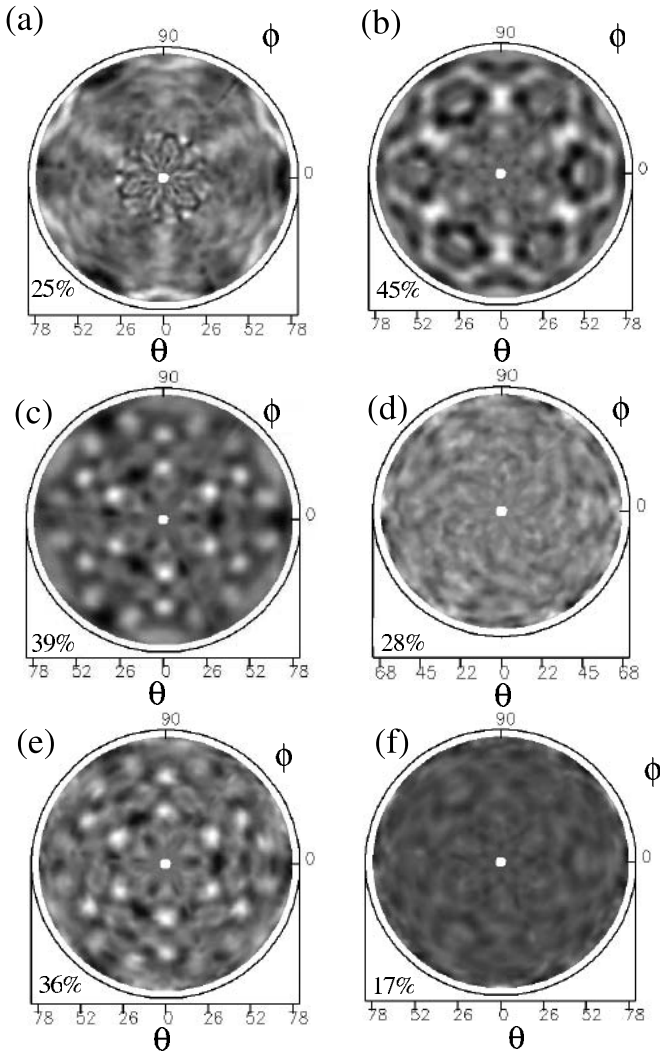

FIG. 5. Experimental photoelectron diffraction patterns for Pd on Ru(0001) at RT, excited with Mg $K\alpha$ radiation for the Pd $3d$ emission peak (KE=918 eV) and for the Ru $3d$ emission peak (KE=973.5 eV) are presented at the right and at the left column, respectively, for 1 ML [(a) and (b)], 5 ML [(c), and (d)] and 15 ML Pd [(e) and (f)].

The theoretical simulations for the XPD patterns were performed by using the MSCD code.[30] The phase shifts for the scattered electrons were obtained using a muffin tin potential for Pd and Ru atoms in their bulk phases. The cluster model has a parabolic shape with 10.5 Å radii and 16 Å depth, which corresponds to approximately 270 atoms in the cluster. The cluster configuration was chosen to allow up to seven emitting layers and avoid boundary effects in the multiple scattering calculations. Since the photoelectrons excited with the Mg $K\alpha$ have high kinetic energies (918 eV for the Pd $3d_{5/2}$ and 973.5 eV for the Ru $3d_{5/2}$), the most significant contribution came from forward scattering which is not very sensitive to the atomic structure of the surface layer, but is very efficient for precisely determining the atomic packing and interlayer distances in a film of several atomic layers. Up to six multiple scattering events were allowed for each emitted electron, which was enough to fully describe the problem. Rotated domains of Pd islands on the surface were

treated by considering a linear combination of the calculated patterns in each domain. The reliability of the theoretical simulations as compared to the experimental data sets was evaluated by the well-established *R*-factor analysis.[30] In this analysis, the lowest R_a factor means a better theory-experiment comparison. In order to refine the selected structural models, we permitted the complete relaxation of the structural parameters (in-layer lattice parameters and interlayer distances) as well as the nonstructural parameters such as the Debye temperature, inner potential, and experimental angular resolution of the analyzer. Due to the large number of parameters to be tested, the multidimensional parameter space could be computationally mapped only by using comprehensive search algorithms which speeded up the calculations. A single pattern simulation takes around 20 min with a single 2.14 Ghz AMD-Opteron 64 bits processor. The computations have been successfully done using the high-performance LNLS personal computer cluster with a MPI parallelized version of the MSCD code.[30] Each simulation used an 8 AMD-Opteron processor subcluster, which speeded up the calculations by a factor of 6.5–7. The search for the best model was carried out using a grid search algorithm combined with a genetic algorithm (GA).[31] The complete structural determination took around 3000 simulations to map the multidimensional parameter space in each model.

The XPD simulations for the low coverage film (0.5–1 ML) confirm qualitatively the diffraction pattern presented in Fig. 5. The combined information obtained from the experiment and the simulations leads us to conclude that Pd forms a flat overlayer on the Ru(0001) surface, showing a diffraction pattern relatively featureless for polar angles below 60° and a sixfold structure at angles around 68°–78°. It supports the conclusion that Pd is only present at the surface without diffusion. The features displayed in the XPD pattern from the Ru 3*d* signal are better reproduced when Pd atoms are occupying the hcp-hollow sites on the substrate. However, the subsequent Pd growing layers follow the conventional fcc packing. From these results, stacking fault packing seems to be unlikely to happen.

In order to describe in detail the atomic structure of the Pd thin films ranging from 5 to 15 ML, several models were considered. The most important models to be tested were a Pd film with the same hcp packing of the substrate (*ABABAB*, …), model 1; a Pd film with fcc packing (*ABCABC*, …) with domains rotated by 60°, model 2; and model 3, corresponding to a zigzag packing produced by stacking faults of the fcc structure (*ABC***B***ABC***B***ABC***B**, …).

Figure 6 exhibits the comparison between the XPD experimental pattern [Fig. 6(a)] of the 5 ML Pd film evaporated at RT and without annealing with the simulated patterns for the three models described above. For each of the models, a full relaxation of the structural and nonstructural parameters was performed. Thus by a direct visual comparison or by using the criterion of the best R_a factor, it was possible to conclude that model 2 is the one which best describes the system. This finding is in perfect agreement with the recent STM results for a submonolayer Pd films on Ru(0001).[25] In their STM analysis, Hoster *et al.*[25] concluded that the first Pd monolayer grows as dendrite islands, which follow the hcp stacking of the substrate, but exhibit two different orientations on the same terrace. Though in that case, it was not possible to decide if the subsequent Pd monolayers assume an hcp or fcc packing. In the present work, we have determined unambiguously that Pd films form fcc structure on Ru(0001).

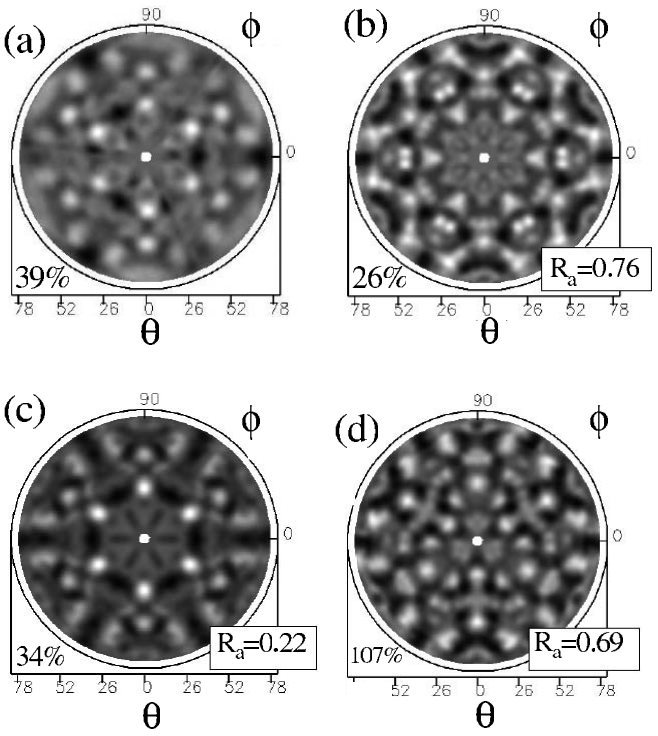

FIG. 6. XPD experiment-theory comparisons for the Pd 3*d* emission from 5 ML Pd as grown on Ru(0001) at RT. (a) Experiment, (b) model 1, (c) model 2, and (d) model 3. The percent indicate the maximum anisotropy of the photoelectron diffraction signal, and R_a is the best reliability factor found after full relaxation of the structural and nonstructural parameters (details in the text).

As with all studies of this type, a very big worry is the choice of the correct models to propose, so it would probably be useful to discuss in greater detail the simulation procedures. In the first attempt to simulate the experimental Pd XPD pattern, we have considered structural parameters fixed to that ones of the bulk values [Ru(0001) and Pd(111)]. With this configuration, it was tested how many emitting layers should be included in the simulation, which provided us with a confirmation of the coverage determined using the methods described in Sec. III. The results are summarized in Fig. 7. To refine the structure determination, it was allowed first a relaxation in the nonstructural parameters such as the analyzer angular resolution, Debye temperature (T_D), and inner potential (V_0). The value found to the analyzer angular resolution was 1.5°, which is in perfect agreement with the expected value defined by construction of the instrument. The determined value for the Debye temperature was 168±30 K, which is a lower value, compared to the tabulated bulk value of Pd ($T_{D\text{bulk}}$=275 K). Nevertheless, this value is in good agreement with previous determinations for Pd(111) surfaces[32] and with the expected value for the surface component of the Debye temperature described approximately by $T_{Dsurface} \approx \frac{1}{\sqrt{2}} T_{Dbulk}$.[33] Finally, the inner potential was fitted to values around 8 eV.

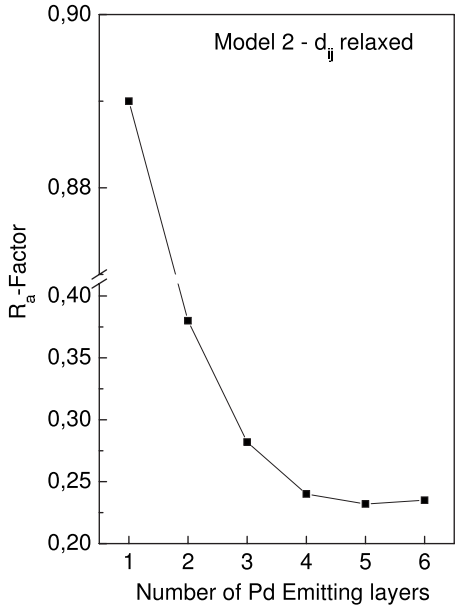

FIG. 7. Reliability factor R_a as a function of the number of Pd emitting layers considering model 2 for the case of 5 ML Pd film.

In a second step, it fixed the nonstructural parameters and mapped the in-plane lattice parameter and the first four interlayer distances. The in-plane lattice parameter was determined to be identical to the Pd(111), i.e., 2.75±0.02 Å. Here, it was not possible to distinguish the development revealed by RHEED. However, the first few interlayer distances showed significant expansions compared to the values displayed by the Pd(111) and the Ru(0001) in their bulk phases. The simulated pattern using fixed bulk interlayer distances for the Pd film produces a R_a factor of 0.34. Permitting a complete relaxation of the first four interlayer distances, it produces a significant reduction in the R_a factor to 0.22 for d_{12}=2.36 Å (first interlayer distance), d_{23}=2.38 Å (second interlayer distance), d_{34}=2.41 Å (third interlayer distance), and d_{45}=2.24 Å (fourth interlayer distance), corresponding, respectively, to 5.2%, 7.0%, 7.4%, and −0.1% expansions and/or contraction relative to the Pd bulk value (2.25 Å). These findings have been confirmed several times by using different starting points and number of generations in the genetic algorithm. The large expansion are surprisingly higher than the values obtained for the Pd(111) single crystal. However, these results can be understood considering that the surface was not annealed and it is formed by rotated islands, which could be accommodating surface tensions between the islands through interlayer expansions.

V. MAGNETISM: EXPERIMENT AND THEORY

Despite the absence of an in-plane lattice expansion, the large relaxation of the interlayer distances observed for the Pd monolayers motivated us to investigate the possibility of induced ferromagnetic properties in such films. The magnetic measurements have been done in the second UHV chamber, by using MOKE.[34] Pd films have been grown with different

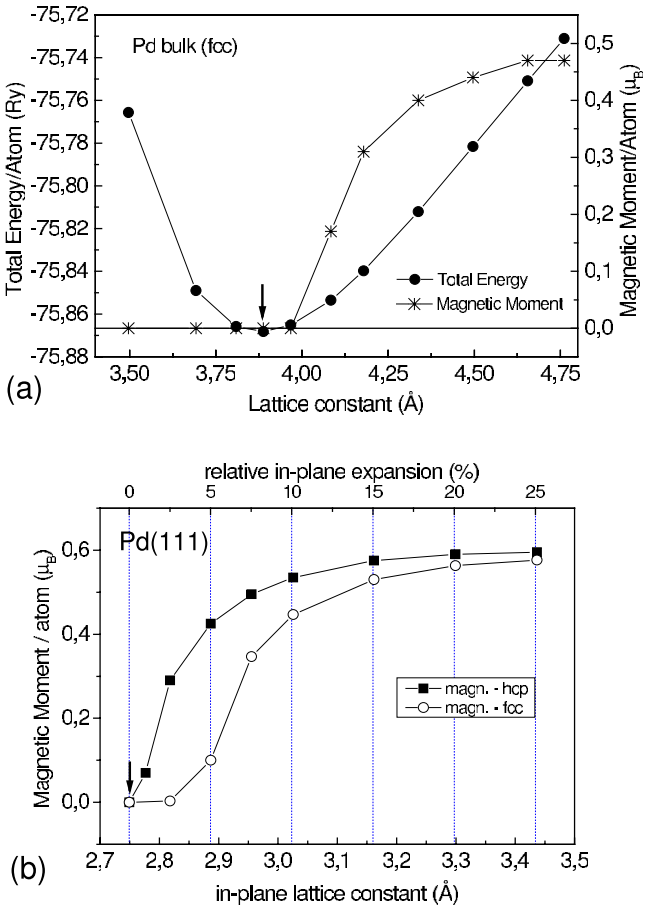

FIG. 8. (Color online) DFT calculation using L(S)DA functional for a fcc Pd and hcp Pd. (a) Total energy (dots) and the magnetic moment (stars) are plotted as a function of the lattice constant in a Pd fcc packing. (b) Magnetic moment for both fcc and hcp packing as a function of the in-plane lattice constant keeping the interlayer distances fixed to the bulk value.

thicknesses from sub-ML up to 15 ML and for substrates at LT and RT.

Longitudinal MOKE experiments were conducted immediately after film growth with the magnetic field applied in the film plane. The MOKE signal was measured with a focused laser beam (λ=670 nm) using *s*-polarized light reaching the film surface at 45° and a crossed polarizer and/or analyzer geometry with the analyzer set at a small angle from extinction. In this configuration, the relative changes of the Kerr intensity are directly proportional to the Kerr rotation and depend both on the longitudinal and polar magnetization components.[35] No hysteretic MOKE loop was observed for Pd films (up to 15 ML) on Ru(0001), as measured at 160 K.

Since the MOKE measurements did not give any evidence of ferromagnetism, we suppose that the expanded films are in a paramagnetic state, contradicting the claim in the literature that an expanded unit cell of Pd induces ferromagnetism.[12] One important question is for what type of expansion this effect happens. To better clarify this question, we conducted our own DFT calculations.

The DFT calculations performed in this work have been done using the Quantum ESPRESSO package[36] and either the

local density approximation (LDA) or the generalized gradient approximation (GGA) to the exchange and correlation terms in the ultrasoft pesudopotentials (USPs). The USPs were exhaustively tested to describe correctly the bulk properties. It has been found that perfect convergence of the self-consistent calculation were obtained considering a cutoff energy of 50 Ry for the wave functions and sampling the Brillouin zone with $12\times12\times12$ k points using the Monkhorst-Pack method.[37] To describe the magnetic order, the linear spin density approximation [L(S)DA][38] was included in the exchange-correction potentials.

It is known that GGA usually describes better the electronic structure and is more accurate and reliable than LDA. Several DFT studies for Pd have been done using GGA functionals.[43] However, as described by Alexandre *et al.* [39,40] and reproduced here, the GGA functional based on the Perdew-Burke-Ernzerhof[41] overestimates the lattice constant for Pd obtaining 3.99 Å or 2.5% larger than the experimental value of 3.89 Å. It also underestimates the bulk modulus of 1.44 Mbar or −19.8% smaller than the value obtained experimentally. In this case, the calculation predicts a ferromagnetic moment of $0.4\mu_B$/atom for the Pd ground state, which is obviously wrong. On the other hand, LDA found the equilibrium (minimum of the total energy) in a paramagnetic state with a lattice constant of 3.89 Å and bulk modulus of 1.8 Mbar, which is in a perfect agreement with experimental results.[42] In short, it seems that GGA functional is not adequate to describe the paramagnetic-ferromagnetic transitions in this system.

Using the LDA functional, we performed calculations considering hcp and fcc packing and varying the lattice parameter, interlayer distance, and intralayer distance to monitor the magnetism of the deformed bulk phases of Pd. Changing the lattice constant for the fcc structure, we found that Pd bulk becomes ferromagnetic for lattice constant expansions above 6% and the magnetic moment saturates in $0.47\mu_B$/atom for expansions above 22%. These results are summarized in the Fig. 8(a). Fixing the interlayer distance to be identical to the Pd bulk (2.25 Å) and relaxing the in-plane lattice parameter, it is possible to see that Pd becomes magnetic for an hcp packing for expansions around 1% and shows larger magnetic moment when compared to the same expansion in the fcc packing [Fig. 8(b)].

We might think that the increase in the volume of the unit cell or only the reduction in the coordination number is correlated to the induced ferromagnetism. Nevertheless, we found that keeping the in-plane lattice parameter, i.e., the nearest-neighbor distance fixed to the Pd bulk value (2.75 Å) and increasing the interlayer distance do not affect the magnetic state of the Pd. The calculations always result in a paramagnetic state, even for interlayer expansions above 20%. This result explains very well the absence of ferromagnetic behavior in our MOKE measurements in Pd/Ru(0001) ultrathin films.

The explanation can be correlated to the population of the d states that depend on the atomic bond distance. For instance, configurations where the first-neighbor distances are equal or smaller than those of Pd bulk (2.75 Å), the Pd d band are broad and with reduced number of states close to the Fermi level. It is due the strong electron-electron interaction that splits the d band. However, for larger atomic bond distances, electron-electron interaction is reduced and d band becomes more atomiclike, narrow, and with a larger density of states near the Fermi energy. Increasing the DOS at the Fermi level fulfills the Stoner criterion in these cases. Figure 9 shows the evolution of the calculated spin-polarized DOS (convoluted with a 0.2 eV Gaussian width) for three cases: (a) fcc bulk, (b) 12% expanded fcc, and (c) 1% expanded hcp. For (b) and (c), the Stoner criterion is satisfied and as is clearly seen the narrowing of the bandwidth and increasing of the DOS at the Fermi energy.

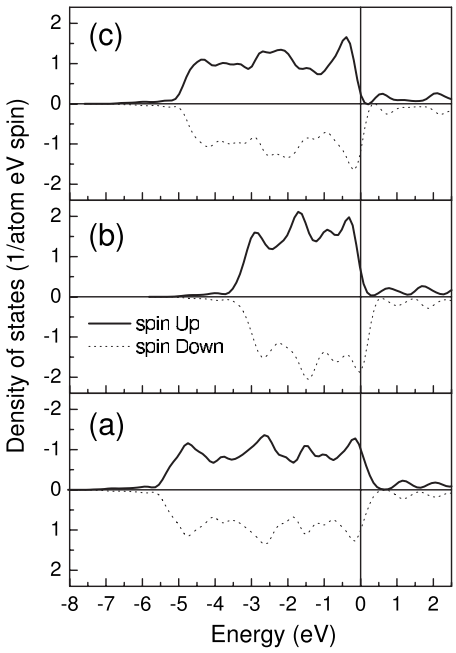

FIG. 9. Calculated Pd spin-polarized density of states for (a) bulk fcc, (b) 12% expanded fcc, and 1% expanded hcp.

VI. CONCLUDING REMARKS

This work addressed in detail the growth process of Pd on Ru(0001) at LT and RT, for film thickness ranging submonolayer up to around 15 ML. The experimental results using a multitechnique approach (XPS, LEED, and RHEED) demonstrate that Pd does not grow in a layer-by-layer fashion, as suggested by previous results in the literature, at least for the experimental conditions described here (room temperature and 160 K growth). A careful XPS investigation of the Pd electronic structure for different film thicknesses, upon annealing from RT to 1000 K, concludes that Pd does not diffuse into the Ru and strongly suggests that even surface alloying does not happen in this system. This finding is also supported by the XPD results and agrees with previous experimental and theoretical work.

Exploring the well-known capabilities of the XPD technique it was possible to determine that Pd grows on Ru(0001) forming 60° rotated fcc domains. For the particular case of 5 ML of Pd as grown, the in-plane lattice parameter was determined to be identical to the Pd(111) bulk parameter.

The interlayer distances show a strong relaxation of about 6% with respect to the bulk Pd, which could reflect accommodations of the surface stress in the domains.

Regarding the magnetic characteristics of these films, it was not possible to identify any signal of ferromagnetism by longitudinal MOKE measurements. DFT calculations show that GGA based on Perdew-Burke-Ernzerhof[38] is not one appropriate functional to described paramagnetic-ferromagnetic transitions in Pd. On the other hand, the LDA functional described the bulk properties and predicted correctly the paramagnetic state for bulk Pd. It also predicts that ferromagnetic bulk Pd is only possible when the atomic bond length is larger than 2.75 Å. For an hcp packing, the magnitude of the lattice expansion necessary to induce ferromagnetic order is substantially reduced.

ACKNOWLEDGMENTS

The authors are pleased to thank LNLS staff for their technical support, especially P. T. Fonseca for his help during the measurements in the SGM beamline. We are in debt with M. L. Viana (UFMG) and E. A. Soares (UFMG) who permitted the use of their GA algorithm. This work received financial support from FAPESP and MCT/CNPq (Brazil).

*Author to whom correspondence should be addressed: FAX: 55 19 3512-1004; abner@lnls.br

[1] J. A. Rodriguez, Surf. Sci. Rep. **24**, 223 (1996).
[2] C. M. Schneider and J. Kirschner, in *Handbook of Surface Science: Electronic Structure*, edited by K. Horn and M. Scheffler (Elsevier, New York, 2000), Vol. 2.
[3] W. A. A. Macedo and W. Keune, Phys. Rev. Lett. **61**, 475 (1988); W. A. A. Macedo, F. Sirotti, G. Panaccione A. Schatz, W. Keune, W. N. Rodrigues, and G. Rossi, Phys. Rev. B **58**, 11534 (1998).
[4] R. Allenspach and A. Bischof, Phys. Rev. Lett. **69**, 3385 (1992); J. Shen, Z. Gai, and J. Kirschner, Surf. Sci. Rep. **52**, 163 (2004); R. D. Ellerbrock, A. Fuest, A. Schatz, W. Keune, and R. A. Brand, Phys. Rev. Lett. **74**, 3053 (1995).
[5] M. A. Tomaz, Tao Lin, G. R. Harp, E. Hallin, T. K. Sham, and W. L. O'Brien, J. Vac. Sci. Technol. A **16**, 1359 (1998).
[6] T. Shinohara, T. Sato, and T. Taniyama, Phys. Rev. Lett. **91**, 197201 (2003).
[7] B. Sanpedro, P. Crespo, A. Hernando, R. Litrán, J. C. Sánchez López, C. López Cartes, A. Fernandez, J. Ramírez, J. González Calbet, and M. Vallet, Phys. Rev. Lett. **91**, 237203 (2003).
[8] E. Hüger and K. Oshch, Thin Solid Films **488**, 291 (2005).
[9] K. Osuch, E. B. Lombardi, and L. Adamowicz, Phys. Rev. B **71**, 165213 (2005).
[10] Y. Yamamoto, T. Miura, M. Suzuki, N. Kawamura, H. Miyagawa, T. Nakamura, K. Kobayashi, T. Teranishi, and H. Hori, Phys. Rev. Lett. **93**, 116801 (2004).
[11] P. Crespo, R. Litrán, T. C. Rojas, M. Multigner, J. M. de la Fuente, J. C. Sánchez-Lopez, M. A. García, A. Hernando, S. Penadés, and A. Fernández, Phys. Rev. Lett. **93**, 087204 (2004).
[12] E. Hüger and K. Osuch, Phys. Rev. B **72**, 085432 (2005).
[13] J. Walter, Adv. Mater. (Weinheim, Ger.) **12**, 31 (2000).
[14] F. Aguilera-Granja, J. M. Montejano-Carrizalez, and R. A. Guirado-López, Phys. Rev. B **73**, 115422 (2006).
[15] (a) E. C. Stoner, Proc. R. Soc. London, Ser. A **165**, 372 (1938); **169**, 339 (1939); (b) A. P. Guimarães, *Magnetism and Magnetic Resonance in Solids* (Wiley, New York, 1998).
[16] A. Steltenpohl and N. Memmel, Phys. Rev. Lett. **84**, 1728 (2000).
[17] A. de Siervo, E. A. Soares, M. F. Carazzolle, R. Landers, and G. G. Kleiman (unpublished); A. de Siervo, Doctorate thesis, University of Campinas, Brazil, 2002.
[18] J. Kolaczkiewicz and E. Bauer, Surf. Sci. **423**, 292 (1999).
[19] T. H. Andersen, Z. Li, S. V. Hoffmann, L. Bech, and J. Onsgaard, J. Phys.: Condens. Matter **14**, 7853 (2002).
[20] S. R. Brankovic, J. MacBreen, and R. R. Adzic, Surf. Sci. **479**, L363 (2001).
[21] J. Fassbender, U. May, B. Schirmer, R. M. Jungblut, B. Hillebrands, and G. Güntherodt, Phys. Rev. Lett. **75**, 4476 (1995); A. de Siervo, R. Paniago, E. A. Soares, H.-D. Pfannes, R. Landers, and G. G. Kleiman, Surf. Sci. **575**, 217 (2005).
[22] M. P. Seah, in *Practical Surface Analysis*, edited by D. Briggs and M. P. Seah (Wiley, New York, 1990), Vol. 1, Chap. 5.
[23] L. Z. Mezey and J. Geber, Jpn. J. Appl. Phys., Part 1 **21**, 1565 (1982).
[24] A. V. Ruban, H. L. Skriver, and J. K. Norskov, Phys. Rev. B **59**, 15990 (1999).
[25] H. E. Hoster, E. Filonenko, B. Richter, and R. J. Behm, Phys. Rev. B **73**, 165413 (2006).
[26] R. A. Campbell, J. A. Rodriguez, and D. W. Goodman, Phys. Rev. B **46**, 7077 (1992).
[27] W. F. Egelhoff, Surf. Sci. Rep. **6**, 253 (1987).
[28] T. H. Andersen, L. Bech, Z. Li, S. V. Hoffmann, and J. Onsgaard, Surf. Sci. **559**, 111 (2004).
[29] W. Olovsson, L. Bech, T. H. Andersen, Z. Li, S. V. Hoffmann, B. Johansson, I. A. Abrikosov, and J. Onsgaard, Phys. Rev. B **72**, 075444 (2005).
[30] Y. Chen and M. A. Van Hove, MSCD, multiple scattering calculation diffraction package, available from http://www.sitp.lbl.gov/mscdpack/mscdpack.html
[31] M. L. Viana, R. Diez Muño, E. A. Soares, M. A. Van Hove, and V. E. de Carvalho (unpublished).
[32] A. de Siervo, E. A. Soares, R. Landers, and G. G. Kleiman, Phys. Rev. B **71**, 115417 (2005).
[33] N. W. Ashcroft and N. D. Mermin, *Solid State Physics* (Saunders, Philadelphia, 1976).
[34] M. D. Martins, L. H. F. Andrade, P. L. Gastelois, and W. A. A. Macedo, J. Appl. Phys. **89**, 6680 (2001).
[35] Z. Q. Qiu and S. D. Bader, J. Magn. Magn. Mater. **200**, 664 (1999), and references therein.
[36] S. Baroni, A. Dal Corso, S. de Gironcoli, P. Giannozzi, C. Cavazzoni, G. Ballabio, S. Scandolo, G. Chiarotti, P. Focher, A. Pasquarello, K. Laasonen, A. Trave, R. Car, N. Marzari, and A. Kokalj, http://www.pwscf.org
[37] H. J. Monkhorst and J. D. Pack, Phys. Rev. B **13**, 5188 (1976).
[38] J. P. Perdew and A. Zunger, Phys. Rev. B **23**, 5048 (1981).
[39] S. S. Alexandre, M. Mattesini, J. M. Soler, and F. Yndurain, Phys. Rev. Lett. **96**, 079701 (2006).

[40] S. S. Alexandre, E. Anglada, J. M. Soler, and F. Yndurain, Phys. Rev. B **74**, 054405 (2006).
[41] J. P. Perdew, K. Burke, and M. Ernzerhof, Phys. Rev. Lett. **77**, 3865 (1996).
[42] C. N. Rao and K. K. Rao, Can. J. Phys. **42**, 1336 (1964); http://www.webelements.com, and references therein.
[43] A. Delin, E. Tosatti, and R. Weht, Phys. Rev. Lett. **92**, 057201 (2004).